

A NOVEL 180° HYBRID BASED ON THE MODIFIED GYSEL POWER DIVIDER

M. Fartookzadeh, S. H. Mohseni Armaki* , and M. Kazerooni

Electrical & Electronic University Complex (EEUC), MAUT, Tehran
15875-1774, Iran

Abstract—A novel 180° hybrid is proposed, based on a modified Gysel power combiner, using phase shifter and ground bridge for the difference output. Also the Defected Microstrip Structure has been used to increase the hybrid's phase matching. All steps of the design are simulated using HFSS 11 and the final design is validated by the fabrication. It has good results between 7 GHz to 10 GHz and can be used between 6 GHz to 11 GHz with less accuracy.

1. INTRODUCTION

Angle error sensing plays a main role of monopulse trackers in radar systems. A monopulse system provides simultaneous comparison between the received signals of its antenna from a target, with elevation and azimuth differences (only one pulse is essential) [1]. Monopulse comparator is a network that can be constructed using only a set of power combiners those are called 180° hybrids (hybrid couplers) and produces sum and difference of its input signals. Each of these power combiners can be a magic-T, a rat-race hybrid, or any other 4-port circuit that generates these two signals. Despite the rat-race hybrid [2], magic-T [2] is not initially designed for the microstrip technology and it is based on the waveguide technology [2], but it is applicable to the microstrip technology. Anyway, for the microstrip technology, the only preferred limitation is that the input ports of the hybrids should be beside each other to allow monopulse comparator be constructed directly (For example the rat-race hybrid doesn't have this feature).

Received 10 January 2012, Accepted 20 February 2012, Scheduled 27 February 2012

* Corresponding author: Seyed Hosein Mohseni Armaki (mohseni@ee.iust.ac.ir).

Also, monopulse comparator networks can be constructed using 90° hybrid, but it usually has less bandwidth. One example is given in [3]. The accuracy, bandwidth, power handling and other characteristics of a monopulse comparator are depended on its involving hybrids. Therefore, new investigations are arising to obtain better 180° or 90° hybrid couplers. For example, in [4] a wideband 90° hybrid is introduced, but the level of bandwidth and accuracy is lower than 180° hybrids. Whilst the microstrip-slotline transition is used twice in [5] to obtain wideband 180° hybrid, this structure doesn't have the preferred limitation and the outputs and inputs are alternatively between each other. So, it is not able to be inserted directly to form a monopulse comparator. Also there are some proposed 180° hybrids that have input ports beside each other like the planar magic-T using 3-layer substrate [6] or the 180° hybrid based on Wilkinson power divider [7] introduced in [8] and developed in [9]. But as the knowledge of the authors, a 180° hybrid that uses Gysel power divider is not achieved yet.

This paper proposes a 180° hybrid based on the modified Gysel power divider [10] suitable for the monopulse comparator. The inconvenience of the Gysel power divider is the narrow bandwidth, but some modifications are applied on the Gysel power divider to meet the advantages of Gysel power divider with wider bandwidth. Some advantages of Gysel power divider/combiner are 1) it can sustain higher power in lower space, 2) it has better response for imbalanced loads and 3) it has easy realizable geometry [10, 11]. In addition, the Gysel power divider has a less sensitivity on the placement of the resistors on the fabrication of the circuit, and usually it has better phase matching. Similar variation between simulated and fabricated designs' resistors placement can cause higher phase difference on the Wilkinson power divider over the Gysel power divider, because one side of each resistor of the Gysel power divider only has to be grounded and its place is not important. Also the other side does not have an exact point such as $\lambda/4$ through a determined line.

Therefore, modifications on the Gysel power divider arise. For example, in recently published journals, modified Gysel power dividers can be found for arbitrary power ratio division and real terminated impedances [12] and for dual-band applications [13].

The evolution of the modified Gysel power divider is shown in Fig. 1. This circuit will be discussed more in the next section. In the third section, the 180° hybrid circuit will be introduced and it will be ameliorated using DMS in the forth section. Finally, the implementation results are given in the last section.

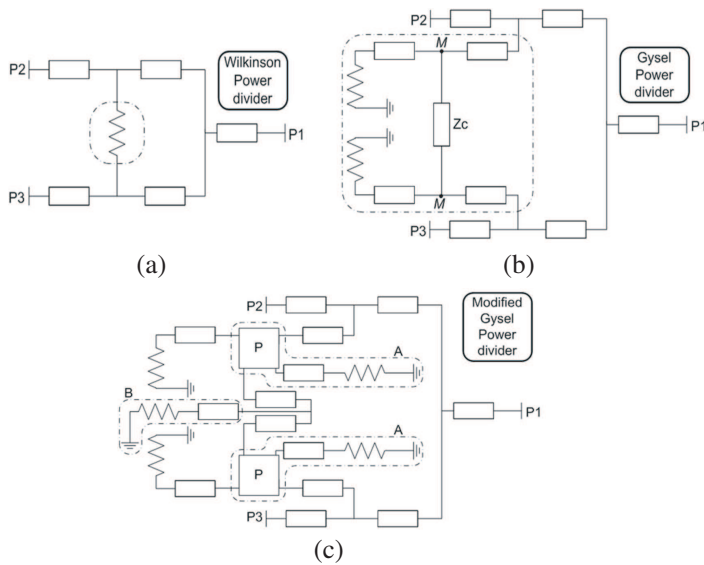


Figure 1. Schematic of (a) Wilkinson, (b) Gysel and (c) the modified Gysel power dividers.

2. THE MODIFIED GYSEL POWER DIVIDER

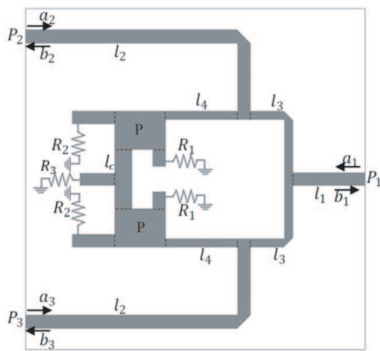
The modifications of the power divider are shown in Fig. 1 explicitly. The line to line resistor of the Wilkinson power divider in Fig. 1(a) is replaced by the known lines and line to ground resistors of the Gysel power divider as shown in Fig. 1(b). In the Gysel power divider the modifications are placed on the point M and at the middle of the connective line Z_C . The point M is replaced by the part A which is a patch coupler, a line and a line to ground resistor as can be seen in Fig. 1(c). Other couplers could be used instead of the patch coupler. It does not defect the results and it can be helpful for the circuit analysis. Part B is placed at the middle of Z_C which are a line and a line to ground resistor. The resulting circuit is shown in Fig. 2(a). This circuit can be implemented on the microstrip explicitly.

The circuit dimensions and values of the resistors are optimized using typical characteristics values of relative dielectric permittivity and loss tangent of a RT/duroid 5870 substrate to the best transmission or insertion loss between 2 GHz to 11 GHz and shown in Table 1. In this table l and w subscripts refer to length and width respectively. Also, return loss is minimized using impedance matching from input to output ports. Isolation is not very important for monopulse

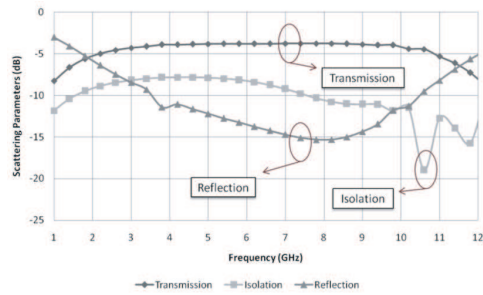
comparator, but it will be seen that the 180° hybrid has an acceptable isolation on its frequency band. Also the isolation of the power divider can be improved using Defected Microstrip Structure (DMS) and Defected Ground Structure (DGS) [14], but here we do not use it because the 180° hybrid does not use all of the power divider’s frequency range and as mentioned it has an acceptable isolation on its bandwidth. Transmission, isolation and reflections of this power divider are shown in Fig. 2(b).

Table 1. Characteristics of the power divider.

Feature	Value	Feature	Value	Feature	Value
ϵ_r	2.33	l_{2w}	0.6 mm	l_{cw}	0.28 mm
<i>loss tangent</i>	0.0012	l_{3l}	7.1 mm	P_l	2.28 mm
h	0.254 mm	l_{3w}	0.3 mm	P_w	1.75 mm
l_{1l}	12.7 mm	l_{4l}	7.7 mm	R_1	20Ω
l_{1w}	0.6 mm	l_{4w}	0.15 mm	R_2	20Ω
l_{2l}	11.9 mm	l_{cl}	6.2 mm	R_{c3}	40Ω



(a)



(b)

Figure 2. Modified Gysel power divider, (a) schematic and (b) simulation results.

3. DESIGN OF THE 180° HYBRID

3.1. 180° Hybrid Circuit Configuration

An explicit circuit for the proposed 180° hybrid is shown in Fig. 3(a). This hybrid is to be used in the monopulse comparator and it is based on Gysel power combiner for the high power application. So, for this microstrip hybrid with two outputs and two inputs these conditions are needed: 1) the inputs (outputs) should be next to each other, 2) each input should be connected directly to each output (with no inductive transformation to assure the high power handling). Therefore, it is necessary to pass one line across the other without making connection between them. It means that there should be a bridge for one line across the other. This bridge can be an air bridge (bond wire), or a line or slotline on some other layer of the circuit.

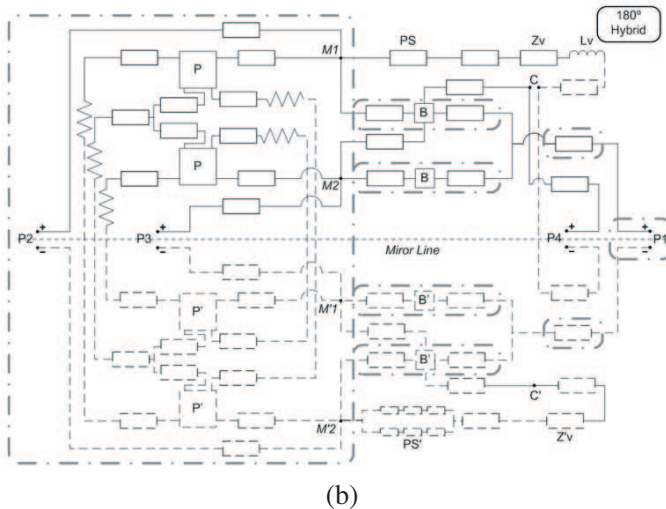
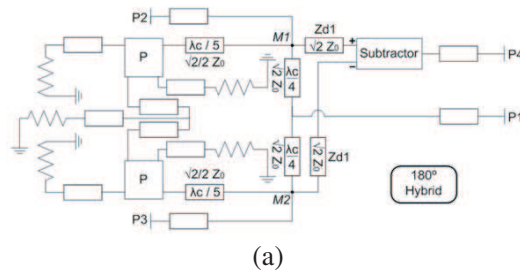


Figure 3. (a) 180° hybrid circuit based on the modified Gysel power-combiner, (b) 180° hybrid double line circuit.

It is known that for a microstrip circuit with a solid ground (single layer circuit), the single line circuit model can be used as used for the power divider. For a double layer circuit or a circuit that uses both sides of the substrate double line circuit model can be more useful. In this method, each line has a corresponding line which shows the return way of the current and the comparative point of the voltage. For a single layer circuit the return line is similar to the main one, so it is usually omitted. It should be considered that the return line can be in the same layer with the main line such as slot lines. Therefore we use a notation for the double line circuits: 1) A mirror line is shown in the circuit; the corresponding return line of each line is mirrored by the mirror line. 2) The lines placed on the ground layer are illustrated with dashed lines. The 180° hybrid double line circuit is, therefore, as shown in Fig. 3(b). The power divider circuit is separated by the dashed lines. It can be seen that the separated lines are similar to their return paths. The microstrip view of this circuit will be given in Fig. 5(a), after introducing the bridges and the subtractor.

This illustration has more details from what we had in Fig. 3(a). For example the bridges or the subtractor are shown in more details. The Phase Shifter (PS) is for the phase adjustment on the point C and the second bridge is for the sum signal (P_1) phase adjustment. More information is given subsequently.

3.2. Ground Bridge

In this structure, the ground bridge is constructed using two vias as its columns. The bridge consists of two short slot lines, but one side of each slotline is directly connected to the lines using vias. The formation of electric field arrows from line to slotline and from slotline to line is sketched in Fig. 4(a). It shows the direction of electric field in the substrate. Although the placement of a line between vias (under the bridge) may cause some dispersion for fields, the effect of this dispersion is less than 0.06 dB on scattering parameters up to 11 GHz.

This bridge can be approximated by an ideal inductor and a transmission line. The value of inductance and phase is depended on the dimensions of bridge and the frequency. The more accurate double line circuit model for the bridge with a line across is shown in Fig. 4(b). In this model Z_1 , Z_2 and Z_3 are related to the line which is across the bridge. The slotline in Fig. 4(a) is divided to four similar parts and each one is named Z_s in the circuit model. L_v and Z_v represent the vias. According to Fig. 3(b) one ground bridge is used to pass the sum line across Δ line with no connection and the second is used to achieve the symmetry of the input signal phases on the sum output (P_1 in Fig. 3(a)).

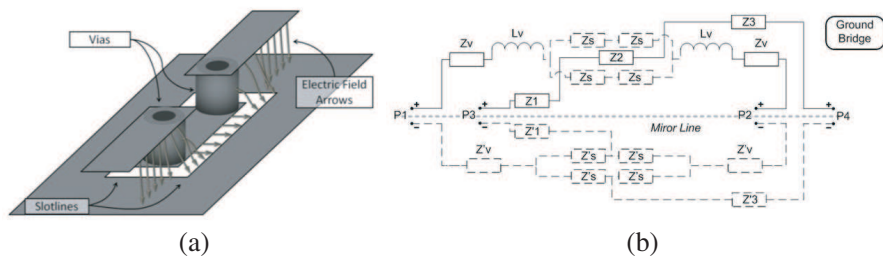


Figure 4. (a) Electric field arrows in substrate in one of the bridge’s slotlines, (b) circuit model for the ground bridge.

3.3. Subtractor and Phase Shifter

Subtractor is what we need on Δ output of the hybrid. This part is actually point C in Fig. 3(b) where one line is converted to ground of the other. This conversion is made using a via from the first line to isolated part of ground near the second line, afterward, the rest of the first line will be a ground for the first line. So the fields of the second line will be subtracted from the first one (or will be added with 180° phase difference), if they were at the same phase at the beginning of line to line comparator. For the waves with similar phases at the inputs, to force them to have same phases at the subtractor point, a simple phase shifter is necessary between M_1 and C in Fig. 3(b). More discussion about the phase shifter will be available after looking at the microstrip view of this circuit in Fig. 5(a).

The phase shifter is to make the current paths of lines equal to each other, or explicitly satisfy

$$\begin{aligned}
 & \int_{\text{width}} \int_{\text{line}} \vec{I}_{s1} \cdot \vec{dl} dw + \int_{\text{path}} \int_{\text{ground}} \vec{I}_{s1} \cdot \vec{dl} dw \\
 &= \int_{\text{width}} \int_{\text{line}} \vec{I}_{s2} \cdot \vec{dl} dw + \int_{\text{path}} \int_{\text{ground}} \vec{I}_{s2} \cdot \vec{dl} dw, \quad (1)
 \end{aligned}$$

where \vec{I}_{s1} and \vec{I}_{s2} are respectively the currents between M_1 and M_2 to the point C in Fig. 5(b). As shown in Fig. 5(b), these integrals can be replaced by three equivalent paths for each line. The path of line has

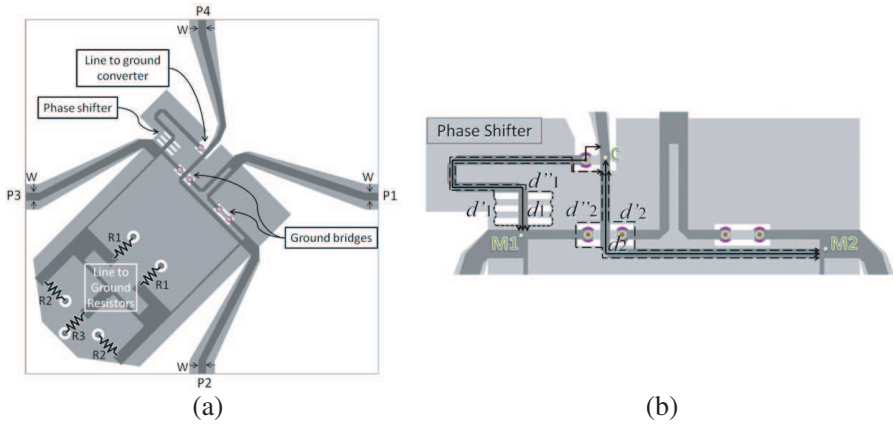


Figure 5. (a) 180° hybrid based on Gysel power combiner and direct line to line comparator, (b) phase shifter.

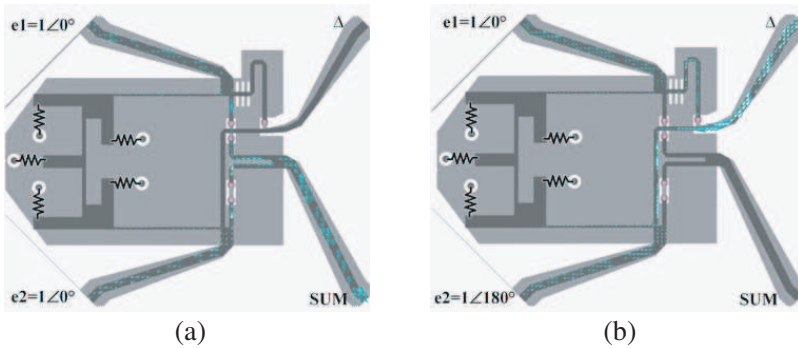


Figure 6. Poynting vectors of the traveling wave on the microstrip lines with (a) equal phases and (b) 180° phase difference, at the inputs.

the same value with the path of ground. So (1) can be replaced by

$$d_1 + \frac{d'_1 + d''_1}{2} = d_2 + \frac{d'_2 + d''_2}{2} \quad (2)$$

The widths of d_1 and d_2 can have primary effect on the amplitudes of voltages at point C, but to have a full control on the amplitudes, length of d_1 and sizes of DGSs can be used. The best size can be obtained from optimization to have same amplitudes and phases on C for same inputs. Consequently, if the waves have similar phases at the input ports, the phase of them will be equal at C, and the difference between voltages of the lines will be zero. So nothing will be sent to P_4 . Also it is obvious that if the inputs have different phases, the

difference will be transmitted to the point C and this variation causes the voltage difference on the lines on this pint so the wave will be transmitted toward P_4 . The maximum power at P_4 will be derived for the 180° phase difference among inputs. It can be seen by the Poynting vectors derived from HFSS in Fig. 6 at 8 GHz.

4. SIMULATION RESULTS

The circuit shown in Fig. 5(a) is simulated using HFSS 11. The results in Fig. 7 appear acceptable between 7 GHz to 10.6 GHz. The phase accuracy is about $\pm 7^\circ$ for the difference output. This inaccuracy has direct effect on the inaccuracy of the null point of the Poynting vector's amplitude. For example as can be seen in Fig. 8, Δ null point deviation of this hybrid is 3° in 9 GHz that confirms the phase inaccuracy in Fig. 7(b). This null point deviation is not necessarily related to the squint angle of the radar antenna, but it causes to have a small signal even if the antenna is exactly towards the target. So the threshold of the detector should be raised and therefore the accuracy of the radar decreases. On the other hand, it can be seen from Fig. 8 that the accuracy of the sum signal is not very important for radar trackers, because they usually works where the input phases' differences are near 0° . Anyway the phase accuracy improvement is the purpose of using the DMS in next section.

5. IMPROVEMENT PERFORMANCE USING DMS

The phase differences of the scattering parameters in Fig. 7(b) offer a clue; both of them is good on about 8 GHz and retreats from its

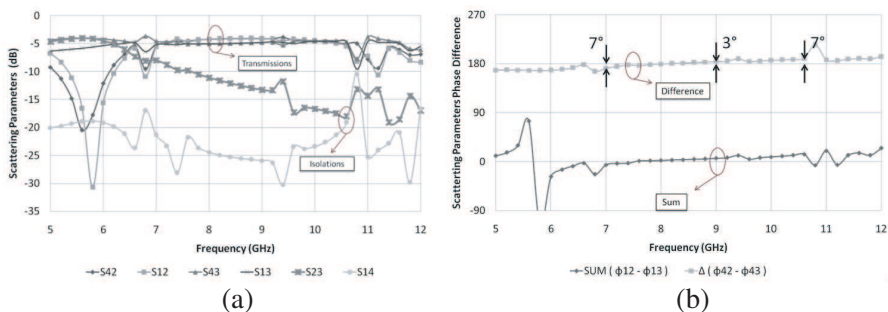


Figure 7. Simulation results of the 180° hybrid, (a) transmission of sum and difference and isolation of inputs and outputs, (b) phase differences.

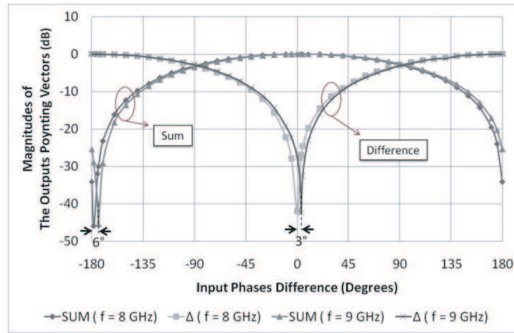


Figure 8. Normalized magnitudes of the sum and difference Poynting vectors.

place toward more phase difference in the same direction by increasing the frequency. Thus, somewhere on the circuit should be found and changed that makes the same variation on the phases differences of the outputs. This is of course, one of the input lines, and the easiest change is to place a DMS on the line. Different shapes of DMS can be utilized to compensate this phase deviation, but the amount of phase change is mostly depended on the size of the DMS; larger DMS brings about more phase difference and generally the DMS causes more phase delay by increasing the frequency, as will be seen subsequently. Therefore and while $(\phi_{12} - \phi_{13})$ and $(\phi_{42} - \phi_{43})$ are rising by the frequency increase DMS should be placed on the line of port 2.

Now we have more degrees of freedom for the phase and amplitude adjustment of the sum and Δ signals. The length of the phase shifter's line and DGS in Fig. 5 and the sizes and positions of The DMS in Fig. 9 are the variables which can improve the phases and amplitudes of the output signals.

It is known that for the monopulse comparator, the accuracy of the phases is more important from the amplitudes and the accuracy of the Δ signal is also more important from the sum signal. So the variables are optimized in order that the deviation of Δ phase difference become as less as possible. As a result, the length of d_1 is 11.15 mm and the size of each slotline of the DGS is $1.7 \text{ mm} \times 0.2 \text{ mm}$, in Fig. 5 and the sizes of the DMS of the input line is given in Fig. 9(a). The amplitudes and phase difference of the initial line and the line with DMS is shown in Fig. 9(b). As can be seen, it may cause about 0.35 dB error in the amplitudes, but the comparison between the phase differences in Fig. 9(b) and Fig. 7(b) indicates that DMS can compensates the deviation in the phase differences of the initial 180° hybrid. However

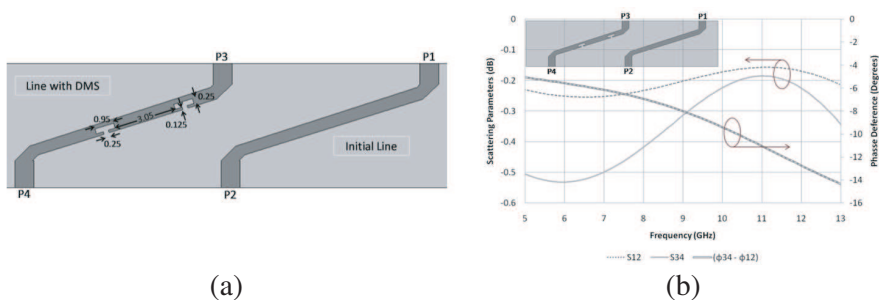


Figure 9. (a) Size and position of the DMS, (b) comparison between results of the lines with and without DMS.

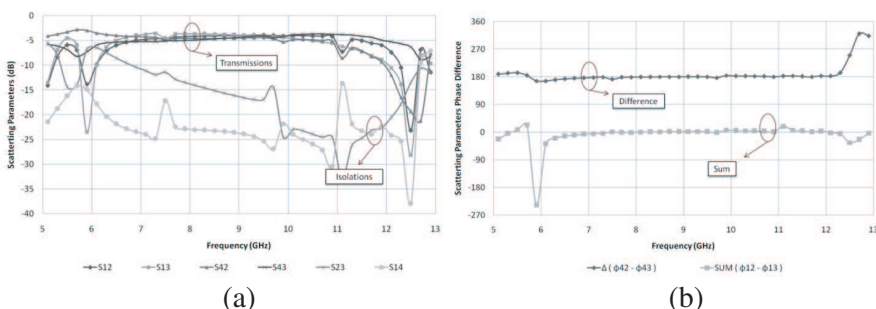


Figure 10. Simulation results of the 180° hybrid with DMS, (a) transmission of sum and difference and isolation of inputs and outputs, (b) phase differences.

the phase difference of Fig. 9(b) begins from about -6.5 degrees at 7 GHz. So the phase shifter of the new 180° hybrid is specified to be larger than the initial one.

The simulation results of the hybrid with DMS (in Fig. 10) shows that it has better phase matching than the initial one (in Fig. 7), and the deviations of the phase differences are completely omitted. It also shows that the transmission and isolation bandwidth is increased by using DMS.

6. IMPLEMENTATION

The simulation results are validated by fabricating the 180° hybrid on a Rogers RT/duroid substrate, as shown in Fig. 11. The dimensions are similar to the simulated circuit. Only the ground under the input

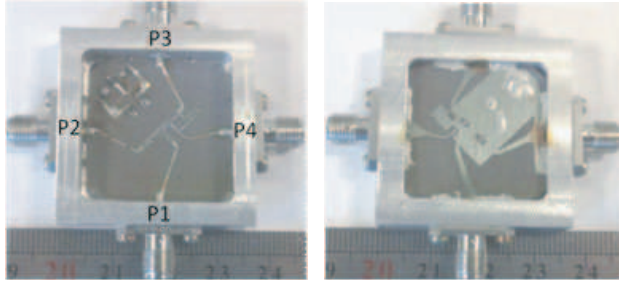


Figure 11. Photograph of the implemented 180° hybrid.

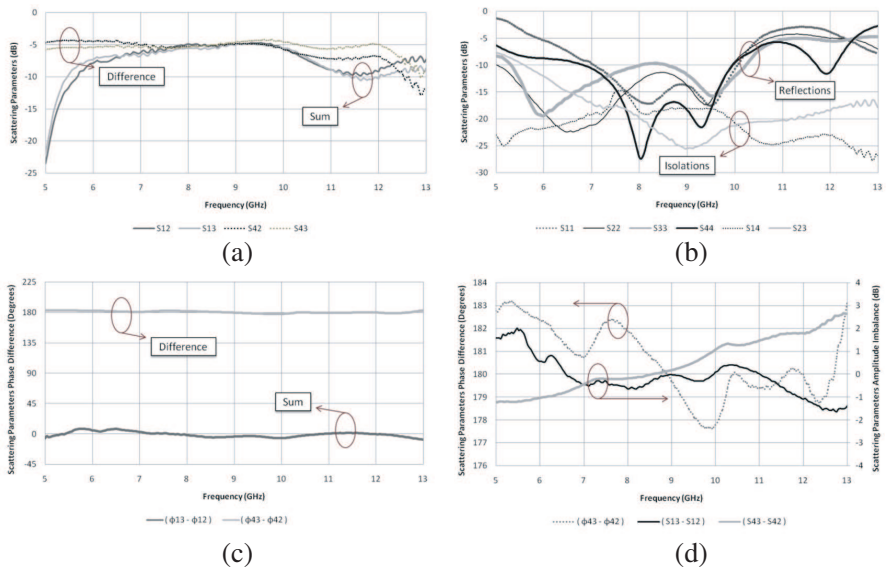


Figure 12. Measurement results, (a) transmissions, (b) isolations and reflections, (c) phase differences, (d) phase differences and amplitudes imbalances.

and output ports are expanded to have a better ground connections. This design is situated in a $2.8\text{ cm} \times 2.8\text{ cm}$ square and the regular monopulse comparator can be made by connecting four copy of it to each other.

Transmissions, isolations and reflections of the hybrid results measured by HP8510 network analyzer are shown in Figs. 12(a) and 12(b). Based on these results, the acceptable bandwidth of the hybrid

is between 7 GHz to 10 GHz, but the phase differences and amplitudes imbalances shown in Fig. 12(c) and Fig. 12(d) shows that it can be used between 6 GHz to 11 GHz if the return loss is neglected. Also it can be seen in Fig. 12(d) that the Δ phase difference deviation is less than 2.3° from 6 GHz to 12.8 GHz.

7. CONCLUSION

A new 180° hybrid based on the modified Gysel power combiner is proposed, which has less than 2.3° Δ phase deviation and less than 1 dB amplitude deviation between 7 GHz to 10 GHz. It uses the ground bridges with two via holes instead of the bound wires to make the fabrication easier and becomes available for commercial uses. This hybrid has a square shape with a wave port at the center of each side. Also, the inputs are directly beside each other, so are the outputs. Therefore, it can be used for monopulse comparator easily. Furthermore, there is a direct connection between both of the inputs and outputs, so the high power handling of the Gysel power divider can be insured more confidently and used for larger monopulse antennas.

REFERENCES

1. Skolnik, M. I. (ed.), *Radar Handbook*, McGraw-Hill, New York, 1970.
2. Pozar, D. M., *Microwave Engineering*, 2nd edition, Wiley, New York, 1998.
3. Wang, H., D. G. Fang, and X. G. Chen, "A compact single layer monopulse microstrip antenna array," *IEEE Trans. Microw. Theory Tech.*, Vol. 54, No. 2, 503–509, Feb. 2006.
4. Chiu, L. and Q. Xue, "Investigation of a wideband 90 hybrid coupler with an arbitrary coupling level," *IEEE Trans. Microw. Theory Tech.*, Vol. 58, No. 4, 1022–1029, Apr. 2010.
5. U-Yen, K., E. J. Wollack, J. Papapolymerou, and J. Laskar, "A broadband planar magic-T using microstripslotline transitions," *IEEE Trans. Microw. Theory Tech.*, Vol. 56, No. 1, 172–177, Jan. 2008.
6. Kim, J. P. and W. S. Park, "Novel configurations of planar multilayer magic-T using microstrip–slotline transitions," *IEEE Trans. Microw. Theory Tech.*, Vol. 50, No. 7, 1683–1688, Jul. 2002.
7. Wilkinson, E. J., "An N-way hybrid power divider," *IRE Trans. Microwave Theory Tech.*, Vol. 8, 116–118, Jan. 1960.

8. Nystrom, G. L., "Synthesis of broad-band 3-dB hybrids based on the 2-way power divider," *IEEE Trans. Microw. Theory Tech.*, Vol. 29, No. 3, 189–194, Mar. 1981.
9. Yang, N., C. Caloz, and K. Wu, "Broadband compact 180° hybrid derived from the Wilkinson divider," *IEEE Trans. Microw. Theory Tech.*, Vol. 58, No. 4, 1030–1037, Apr. 2010.
10. Gysel, U. H., "A new N -way power divider/combiner suitable for high-power application," *IEEE MTT-S Int. Microw. Symp. Dig.*, Vol. 75, 116–118, May 1975.
11. Knochel, R. and B. Mayer, "Broadband printed circuit 0°/180° couplers and high power inphase power dividers," *IEEE MTT-S International Microwave Symposium Digest*, Vol. 1, 471–474, Technische Universitat Hamburg-Harburg Arbeitsbereich Hochfrequenstechnik Postfach 90 14 03, D-2100 Hamburg 90, West Germany, 1990.
12. Wu, Y., Y. Liu, and S. Li, "A modified Gysel power divider of arbitrary power ratio and real terminated impedances," *IEEE Microwave and Wireless Components Letters*, Vol. 21, No. 11, 601, Nov. 2011.
13. Sun, Z., L. Zhang, Y. Liu, and X. Tong, "Modified Gysel power divider for dual-band applications," *IEEE Microwave and Wireless Components Letters*, Vol. 21, No. 1, Jan. 2011.
14. Tirado-Mendez, J. A. and H. Jardon-Aguilar, "Comparison of defected ground structure (DGS) and defected microstrip structure (DMS) behavior at high frequencies," *2004 Proceeding of 1st International Conference on Electrical and Electronics Engineering*, 7–10, Acapulco, Mexico, Sep. 8–10, 2004.